AD-A055 749 ROCKWELL INTERNATIONA_ ANAHEIM CA ELECTRONICS RESEAR--ETC F/G 9/1
ELASTIC WAVE TRANSDUCERS FOR GARNET FIBERS.(U)
SEP 77 D B ANDERSON, R R AUGUST, J E COKER N00173-76-C-0315
UNCLASSIFIED C77-329/501 NL

| OF |
AD
A055749

END
DATE
FILMED
8 -78
DDC

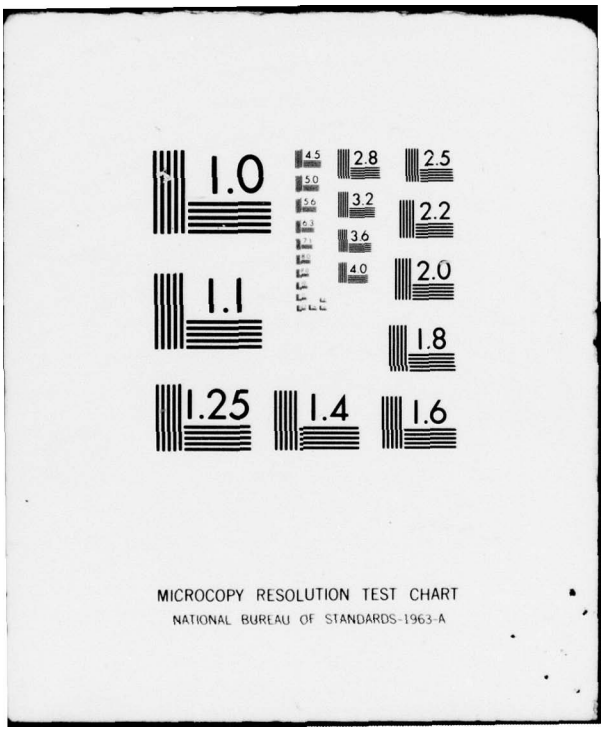
1.0
1.1
1.25
1.4
1.6
1.8
2.0
2.2
2.5
2.8
3.2
3.6
4.0
4.5
5.0
5.6
MICROCOPY RESOLUTION TEST CHART
NATIONAL BUREAU OF STANDARDS-1963-A

FINAL TECHNICAL REPORT

ELASTIC WAVE TRANSDUCERS FOR GARNET FIBERS

D. B. Anderson
R. R. August
J. E. Coker

September 30, 1977

Prepared for the Naval Research Laboratory
Contract No. N00173-76-C-0315

Rockwell International Corporation
Electronics Research Center
3370 Miraloma; Anaheim, CA 92803

C77-329/501

FINAL TECHNICAL REPORT

ELASTIC WAVE TRANSDUCERS FOR GARNET FIBERS

D. B. Anderson
R. R. August
J. E. Coker

September 30, 1977

Prepared for the Naval Research Laboratory
Contract No. N00173-76-C-0315

Rockwell International Corporation
Electronics Research Center
3370 Miraloma; Anaheim, CA 92803

Unclassified

SECURITY CLASSIFICATION OF THIS PAGE *(When Data Entered)*

REPORT DOCUMENTATION PAGE

READ INSTRUCTIONS BEFORE COMPLETING FORM

1. REPORT NUMBER: C77-329/501	2. GOVT ACCESSION NO.
3. RECIPIENT'S CATALOG NUMBER	
4. TITLE *(and Subtitle)*: Elastic Wave Transducers for Garnet Fibers	5. TYPE OF REPORT & PERIOD COVERED: Final Technical Report 9/21/76 to 9/30/77
	6. PERFORMING ORG. REPORT NUMBER: C77-329/501
7. AUTHOR(s): D. B. Anderson, R. R. August, J. E. Coker	8. CONTRACT OR GRANT NUMBER(s): N00173-76-C-0315
9. PERFORMING ORGANIZATION NAME AND ADDRESS: Rockwell International Corporation, Electronics Research Center, 3370 Miraloma; Anaheim, CA 9 2803	10. PROGRAM ELEMENT, PROJECT, TASK AREA & WORK UNIT NUMBERS
11. CONTROLLING OFFICE NAME AND ADDRESS: Contracting Officer Code 5570 gi'allorenzi' Naval Research Laboratory Washington, D.C. 20375	12. REPORT DATE: September 30, 1977
	13. NUMBER OF PAGES: 17
14. MONITORING AGENCY NAME & ADDRESS*(if different from Controlling Office)*	15. SECURITY CLASS. *(of this report)*: Unclassified
	15a. DECLASSIFICATION/DOWNGRADING SCHEDULE: None

16. DISTRIBUTION STATEMENT *(of this Report)*

Distribution of this document is unlimited. Reproduction in whole or in part is permitted for any purpose of the United States Government; Approved for Public release.

17. DISTRIBUTION STATEMENT *(of the abstract entered in Block 20, if different from Report)*

18. SUPPLEMENTARY NOTES

19. KEY WORDS *(Continue on reverse side if necessary and identify by block number)*

Elastic Wave Garnet Fibers

20. ABSTRACT *(Continue on reverse side if necessary and identify by block number)*

The results of an effort to fabricate elastic wave transducers for use on the end of garnet fibers is reported herein. Essential properties for the materials under consideration, namely, fibers and piezoelectric transducers, are included as background together with exposition pertaining to the various types of modes which may be propagated as elastic waves along cylindrical fibers. The transducer design approach considered is described.

DD FORM 1 JAN 73 1473 EDITION OF 1 NOV 65 IS OBSOLETE

Unclassified

SECURITY CLASSIFICATION OF THIS PAGE *(When Data Entered)*

Observations are noted for the gadolinium gallium garnet fibers supplied via NRL from another contractor. The fibers supplied represent a new crystal growth technology which exhibit various kinds of defects which prevented their use. This report documents the various problems encountered.

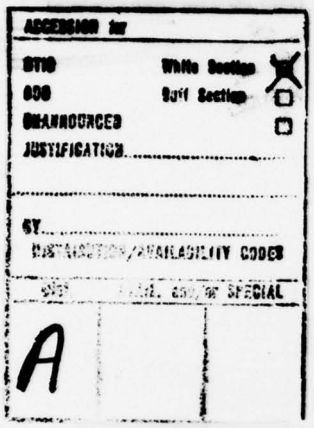

ELASTIC WAVE TRANSDUCERS FOR GARNET FIBERS

By: D. B. Anderson
R. R. August
J. E. Coker

INTRODUCTION

Various signal processing systems continue to require temporary storage for analog and digital information which has ever increasing time-bandwidth-product requirements. The use of elastic waves in bulk and single crystals and surface elastic wave delay lines is employed for temporary data storage. Folding of the propagation path has been necessary to obtain long delays to conserve the size of the single crystal.

By analogue to optical fibers, consideration is now being given to elastic wave propagation in capillary[1] and cladded[2] fibers to implement very long delay lines. Rayleigh waves on the capillary interior surface have been demonstrated. Radial-like and torsional-like waves have been excited at the interface between the cladding and core of Ti-doped fused silica filters. Cladding is used to isolate the particle motion to the interface to minimize the losses. The elastic wave losses of crystals of the garnet[3] and sapphire[4] families exhibit much lower losses which permits their use at higher frequencies.

To exploit higher frequencies, small diameter fibers are required together with the means to implement the necessary transducers. The adaption of existing deposition processes, and lithography for use with these fibers in the high frequency regime, constitutes the objective of this proposed effort. The formation of transducers on the end of cladded and uncladded gadolinium gallium garnet (G^3) fibers supplied by NRL using an oriented zinc oxide thin-film with the appropriately shaped metal electrodes constituted the specific task.

BACKGROUND

Elastic waveguide as circular fibers support three types of modes, namely, torsional, radial and longitudinal.[3,4] The particle displacement of torsional and radial modes is largely shear in nature with orthogonal polarization. To obtain long delays in fibers with a minimum length, the shear-like modes should be employed because the velocity is substantially less than that of the longitudinal wave.

The elastic wave velocities, impedance and absorption for various materials which can be formed as fibers are listed in Table I.[5-9] These parameters apply for the unbounded elastic wave in the medium. For the cladded fiber with wavebinding to the core, the shear velocity of the core must be less than that of the cladding. The resulting torsional or radial modes thus fall between these two limits.

TABLE I

ELASTIC WAVE PROPERTIES FOR SELECTED MATERIALS[5-9]

Material	Velocity (Km/sec)		Impedance (10^6Kg/sec m^2)		Absorption (dB/cm)		Electromechanical Coupling		
	Longitudinal	Shear	Longitudinal	Shear	α_{Long}	α_{Shear}	K_{Long}	K_{Shear}	$K_s \mid \theta$
Fibers									
Fused SiO_2	5.96	3.76	13.1	8.29	15.	20.		---	
Al_2O_3 (c)	11.03	6.78/5.72	43.8	26.9/22.7	0.25	0.5		---	
$Y_3 Fe_5 O_{12}$[001]	7.21	3.84	37.2	19.8	1.7	0.35		---	
$Y_3 Al_5 O_{12}$[001]	8.56	5.03	39.0	22.9	0.4	0.35		---	
$Y_3 Ga_5 O_{12}$[001]	7.08	4.06	40.9	23.5	1.2	0.25		---	
$Gd_3 Ga_5 O_{12}$[001]	6.35	3.57	44.	25.2	0.65	1.2		---	
Electrodes									
Ag [001]	3.44	2.09	36.1	21.9				---	
Al [001]	6.35	3.25	17.2	8.2	75			---	
Au [001]	3.21	1.47	61.3	28.4	200			---	
Piezoelectric Films									
ZnO	6.4	2.88	36.0	15.5			.28	.26	.32 | 43°
CdS	4.46	1.76	21.5	8.5			.15	.19	.21 | 40°

The lowest order azimuthal uniform torsional-like[10] mode is depicted in Figure 1. The corresponding lowest order azimuthal uniform radial-like mode is depicted in Figure 2. This radial-like mode resembles a circumferential Rayleigh wave. It should be noted that the Rayleigh wave contains both longitudinal and shear components in spatial quadrature. The lowest order flexural-like mode is depicted in Figure 3. It also resembles a radial-like mode with the next higher azimuthal order (one circumferential cycle). Each of these modes, torsional, radial and flexural, are depicted as particle displacement at the core-cladding interface where the cladding is assumed to be of infinite extent. The amplitude of the particle displacement is plotted radially for each of the modes. The Bessel functions describe the elastic field amplitude in the core with evanescent decay extending into the cladding. The "-like" nomenclature is employed to indicate that mixing occurs between all of the displacement components except at cut-off and in the infinite radius limit equivalent to a plate. The elastic field amplitude evanescent decay in the cladding permits its thickness to be reduced on the order of a few wavelengths without affecting the loss.

These illustrations of elastic wave modes in fibers are included to indicate the requirements of the transducer displacement to excite and detect these waves. Note that each of these modes require a shear component appropriately arranged relevant to the fiber. The longitudinal modes have not been illustrated because of their larger velocity and because of their much larger loss. Cladding of finite thickness does not provide isolation of particle displacement at the core-cladding interface; i.e., longitudinal mode amplitudes extend to the exterior cladding boundary.

Elastic wave transducers which must function at high frequencies require thickness on the order of the elastic wavelength. For the case at hand, this thickness is approximately 3 microns which requires the deposition of a thin piezoelectric film. Zinc oxide and CdS may be deposited by various techniques with sufficient systematic crystalline orientation to function as piezoelectrics. Their properties are also indicated in Table I. The application of an electric field along the hexagonal or c-axis generates longitudinal stress both along this axis and radially in the plane perpendicular to it. The application of an electric field in any direction perpendicular to the c-axis will generate a shear stress in the plane containing the electric field direction and the crystalline c-axis. The angular functional dependence of the electro-mechanical coupling for ZnO is illustrated in Figure 4. It should be noted that pure longitudinal coupling is achieved for angles of 0° and 63° between the electric field and the c-axis. Pure shear coupling is achieved when these angles are 39° and 90°. Therefore, it is essential that the processing technology be able to control the c-axis orientation relative to the electric field, so as to emphasize a selected type of coupling and its polarization. Techniques have been developed to achieve this orientation.[11-23]

Elastic wave transducer electrode structures to produce various types of modes are illustrated in Figure 5. Disc electrodes containing the piezoelectric are illustrated in the c-axis orientation and the electric field. Section (a) of Figure 5 illustrates a longitudinal mode transducer which may be coupled to the end of the elastic wave fiber. These elec-

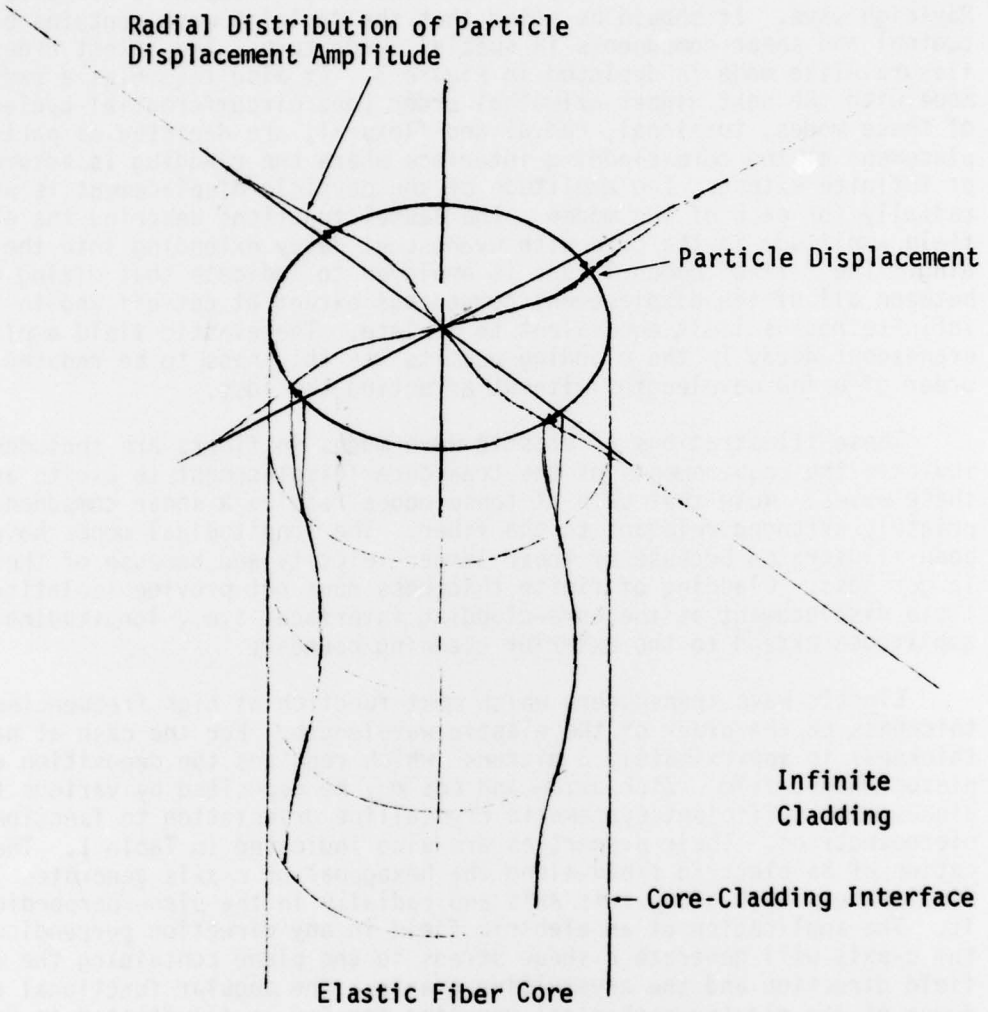

Figure 1. Particle Displacement of Torsional-Like First Order Mode (T_{01}) in Elastic Fiber.

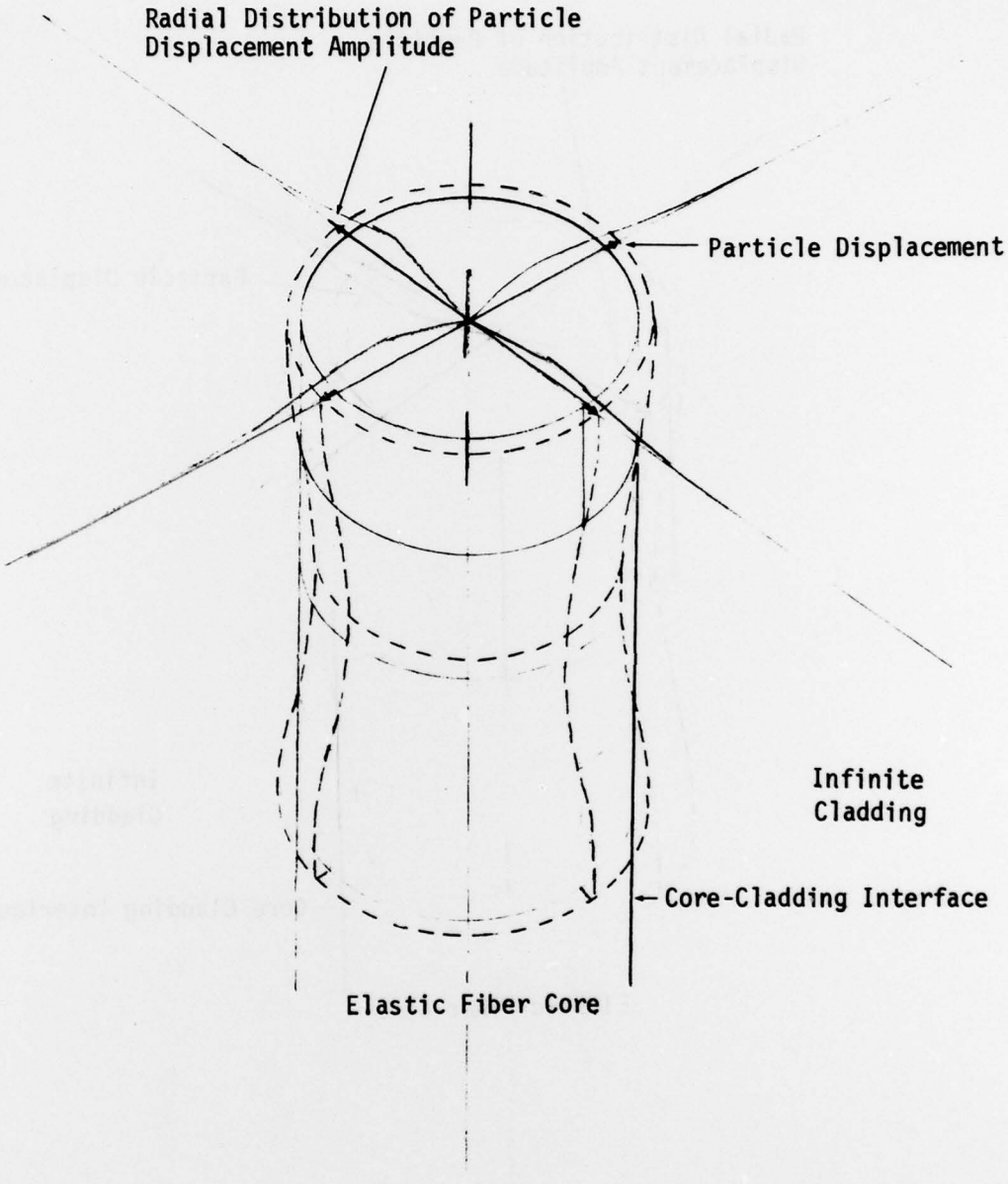

Figure 2. Particle Displacement of Radial-Like First Order Mode (R_{01}) in Elastic Fiber.

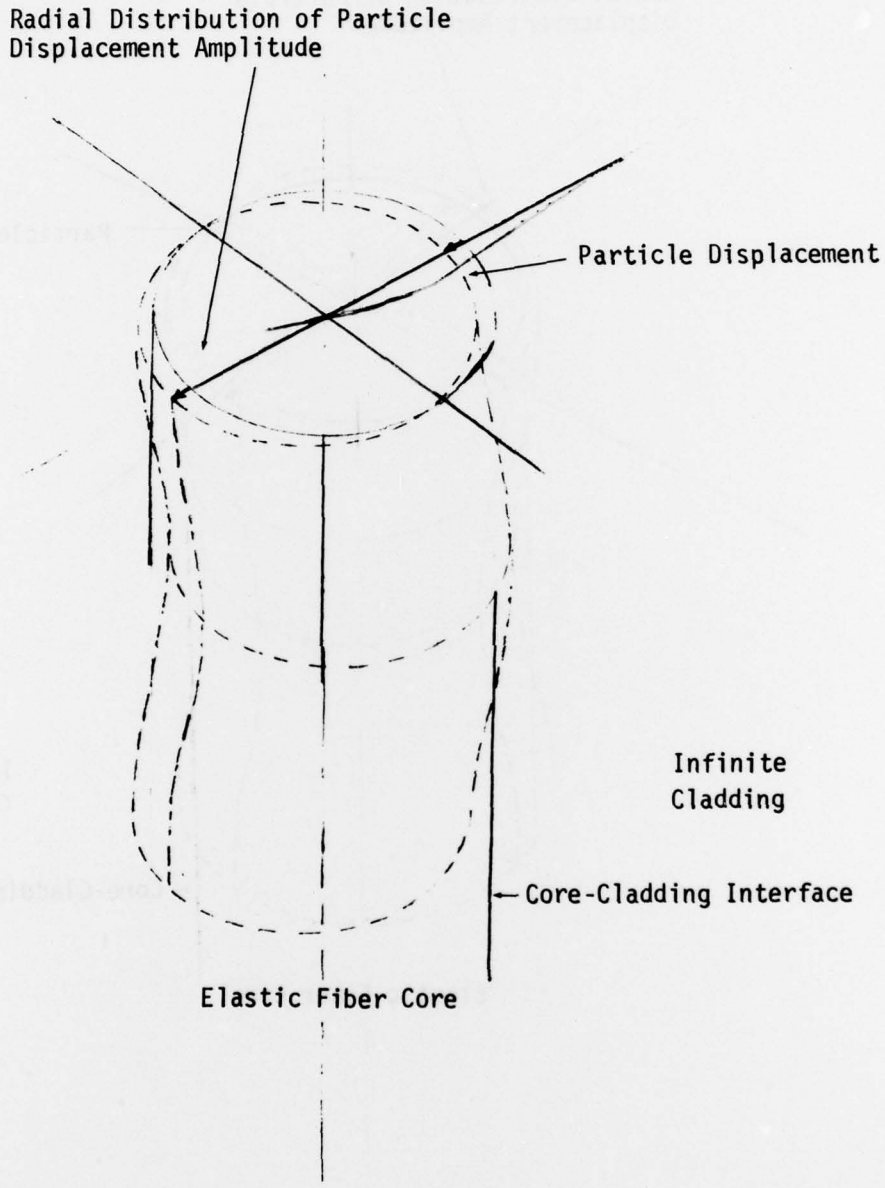

Figure 3. Particle Displacement of Flexural-Like First Order Mode (F_{01}) in Elastic Fiber (Radial-Like First Order Mode with Azimuthal First Order Variation).

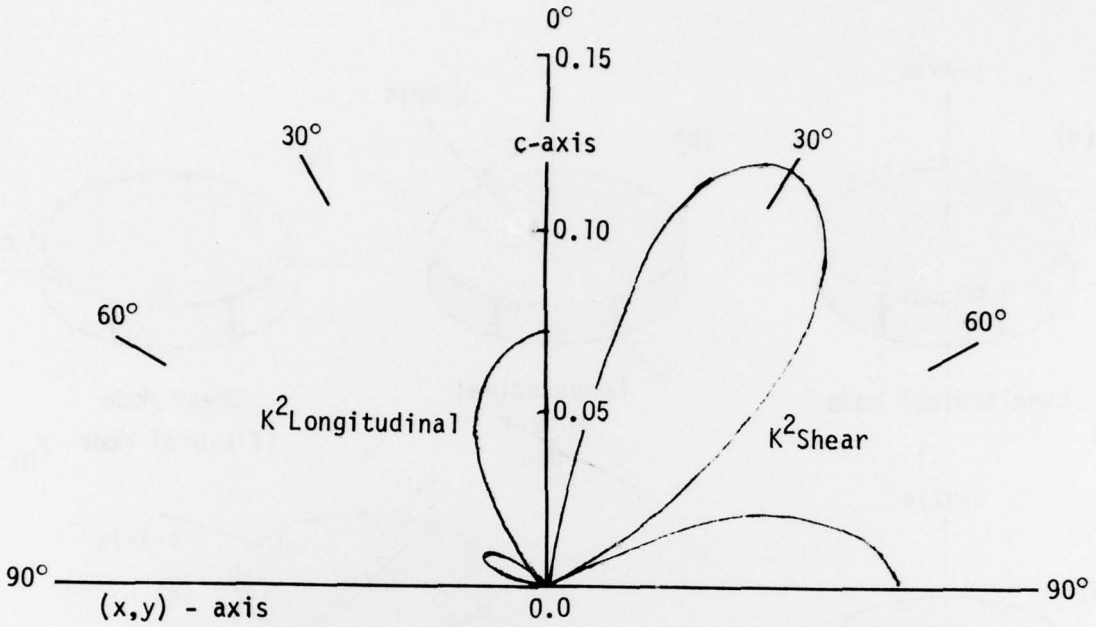

Figure 4. Electromechanical Coupling of ZnO for Longitudinal and Shear Waves Polarized in the Plane Defined by k-vector and c-axis

trodes provide the means to control the radial and circumferential electric field distribution. Because elastic energy must be coupled from the piezoelectric to the fiber by the electrodes, the thicknesses of the electrodes enter into the coupling efficiency and its bandwidth. The thickness of these electrodes must be comparatively thin relative to the elastic wavelength, or may be designed for impedance matching as elastic wave transmission lines using quarter- or half-wave section.[5,12]

Section (c) of Figure 5 depicts the orthogonal orientation producing the shear stress. Section (b) indicates the control of the stress field by the crystalline axis orientation as prescribed in Figure 4. Sections (d), (e) and (f) of Figure 5 indicate a split electrode so that the electric field may have an odd transverse distribution. The configuration depicted in Section (e) will produce a radial mode and the configuration in Section (f) will produce a torsional mode. Because of the split electrode geometry, these transducers will largely excite the R_{11} and T_{11} with azimuthal variations and will partially excite the uniform azimuthal R_{01} and T_{01} modes.

It should be noted that the electrode configuration in Section (a) also has a radial expansion. This component will couple to the R_{01} mode, whereas, the longitudinal component will couple to the L_{01} and R_{01} modes. Further, the electrode configuration in Section (c) will couple to the flexural mode F_{01}. The electrode configuration in Section (d) will excite the L_{11} mode while its radial components will excite the F_{01} mode. The electrode configuration in Section (a) also has a radial expansion. This component will couple to the R_{01} mode, whereas, the longitudinal component will couple to the L_{01} and R_{01} modes. Further, the electrode configuration in Section (c) will couple

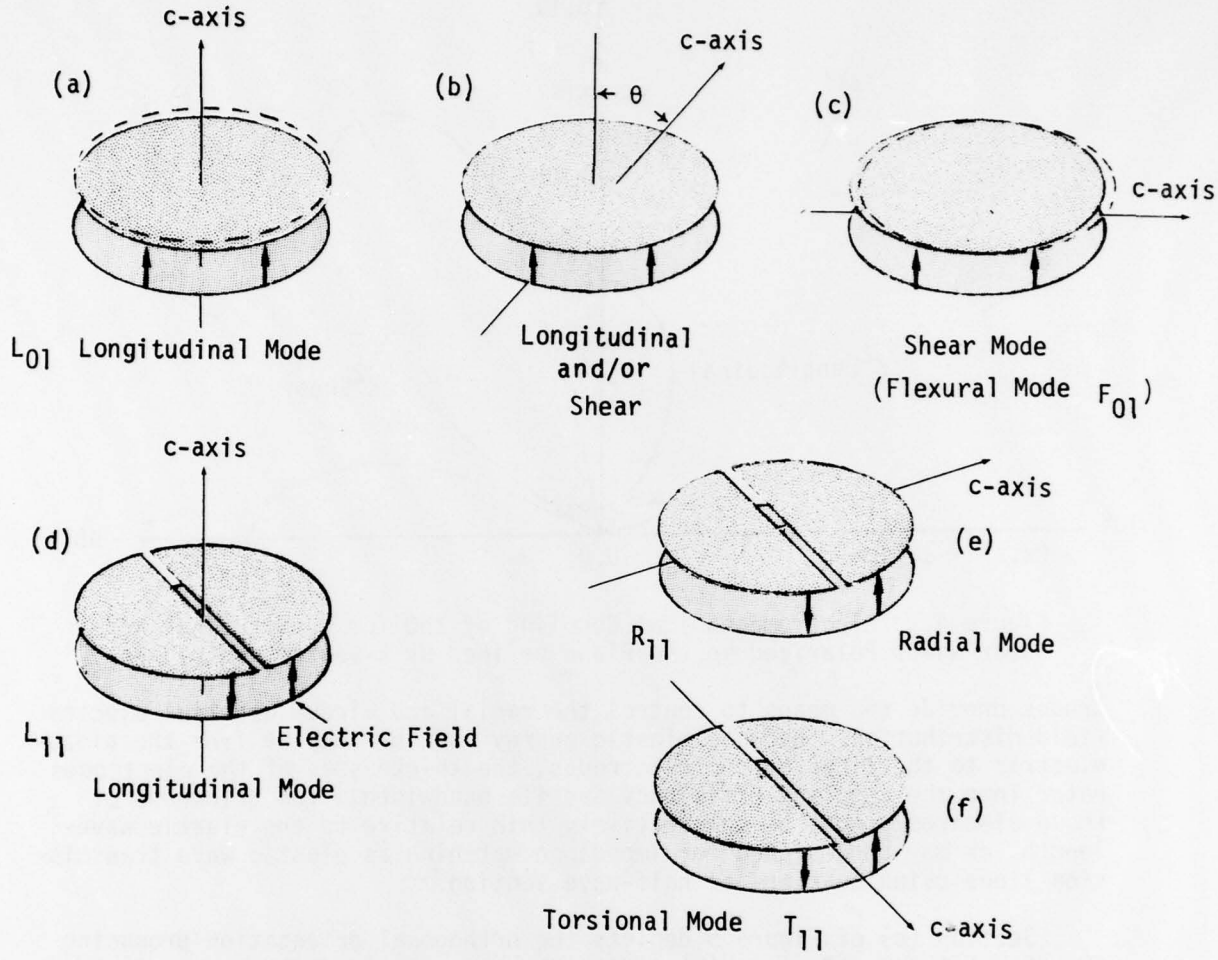

Figure 5. Elastic Wave Transducer Electrode Structures to Produce (a) Longitudinal Mode, (b) Longitudinal or Shear, or both Modes, (c) Shear Mode (Flexural Mode), (d) Higher Order Longitudinal Mode, (e) Radial Mode, (f) Torsional Mode

to the flexural mode F_{01}. The electrode configuration in Section (d) will excite the L_{11} mode while its radial components will excite the F_{01} mode.

APPROACH

The physical implementation of an elastic wave transducer adapted to excite any of these elastic waveguide modes in a cladded fiber is illustrated in Figure 6. It would be delineated by following the process sequence for its implementation. Small fused silica wafers seem to be the most appropriate rigid substrate to attach the cladded elastic fiber, transducer electrodes and electrical terminals. A small diameter hole may be ultrasonically drilled in the wafer for insertion of the fiber and bonding with an epoxy.

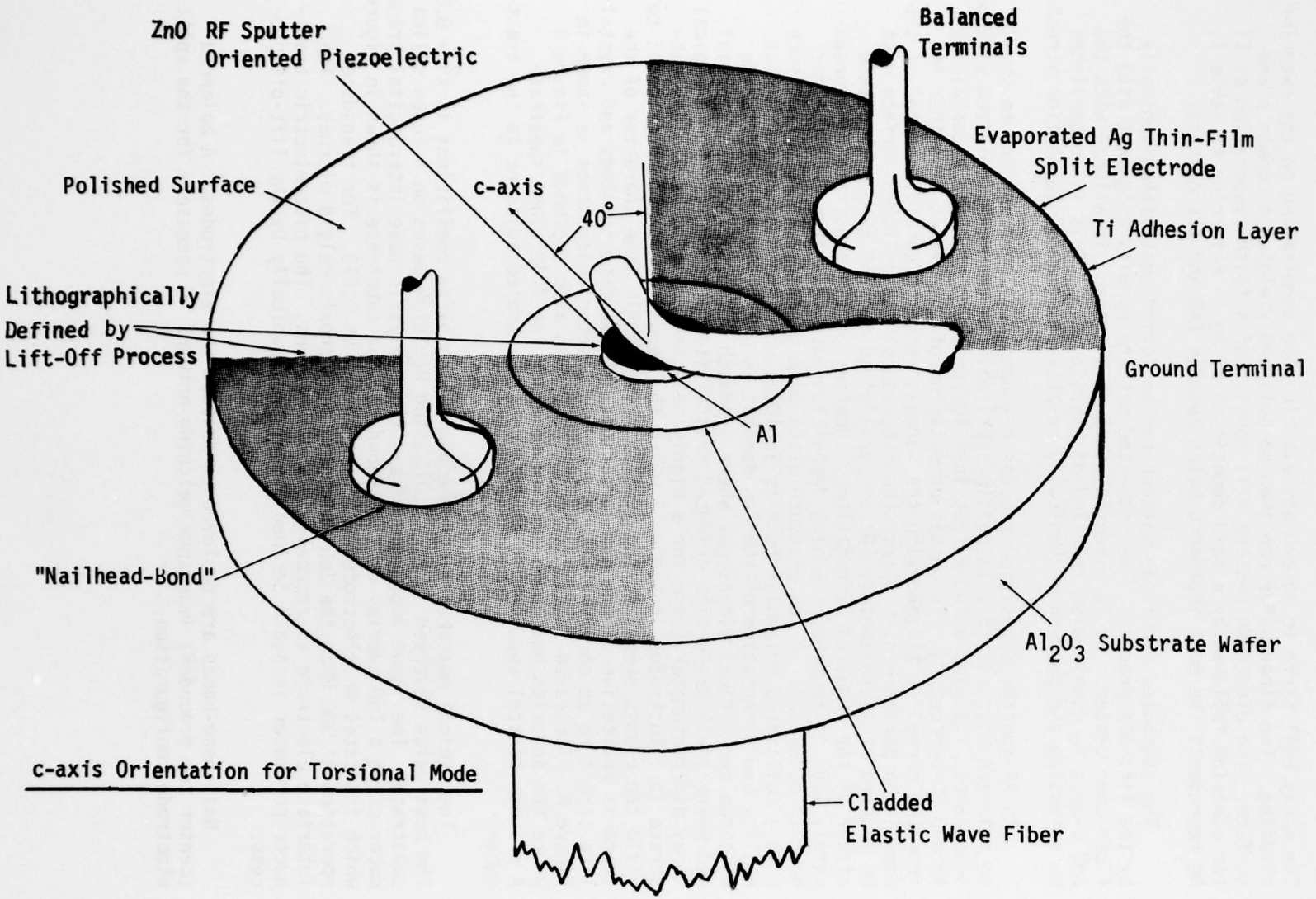

Figure 6. Elastic Wave Transducer Structure for Garnet Fibers

The epoxy will serve to absorb any elastic mode terminating on the exterior cladding. The fiber-wafer can then be polished yielding a common plane surface. The electrode pattern will consist of a flash evaporation of Ti for adhesion followed by a thin deposition of Ag.[17] Referring to Table I, Ag represents the best impedance match between ZnO and the garnets.

The segmented electrode pattern can be formed photolithographically by the lift-off process. The segmented pattern permits alignment with the fiber core center. It is essential that this segment is aligned with the ZnO c-axis to distinguish the kind of elastic mode. This is accomplished by orienting the pattern mechanically relative to the ZnO deposition stream.[16,21]

An RF-sputter deposition process has been developed for ZnO to obtain an oriented piezoelectric thin-film applicable to thermally-oxidized silicon substrates. It uses a ZnO target in a low-pressure atmosphere containing Ar and 20 percent O_2. To obtain orientation of ZnO c-axis at either 40° from the normal or aligned with the normal, requires careful control of the deposition parameters.[14] First the fiber-substrate polished surface must be mounted at approximately 50° or parallel to the ZnO target to obtain either of the required orientations. Heating of the substrate to approximately 150° is required. A slow deposition rate less than 1 micron per hour is essential. A low pressure ultra-pure discharge is required, such that a collimated molecular beam is incident upon the substrate.[16,21] The quality and orientation of the ZnO deposit is established by scattering electron and optical microscopy where a smooth dense surface is essential and where small grain-size oriented crystallites are observed.[14] A typical x-ray diffractometer trace for a highly oriented ZnO film on a glass substrate is illustrated in Figure 7 where the deposition has been oriented to yield the c-axis normal to the surface. The single lobe character of the trace is indicative of the high ordering. The surface topology and crystallite structure as observed with a scanning electron microscope is shown in Figure 8. A cleaved section through the ZnO is also included in Figure 8 where the deposits have been applied to a Corning 7440 glass substrate. A process control specimen is simultaneously executed adjacent to the transducer.

The typical measured electromechanical coupling coefficient is $k^2 = 0.01$. The best value observed is $k^2 = 0.015$ using Rayleigh waves on a fused silica substrate. The input impedance of a surface elastic wave interdigital transducer using a ZnO overlay on the transducer and substrate is shown in Figure 9 which indicates an electromechanical coupling of 0.015. For transducer operation at 300 MHz, the ZnO thickness is approximately 3 microns. The interface electrode is approximately 0.1 microns. The piezoelectric transducer perimeter is again defined photolithographically by the lift-off process.

Nail head-bonds are employed to contact the electrodes. A balanced (center tap grounded) impedance matching network is necessary for the split electrode configuration.

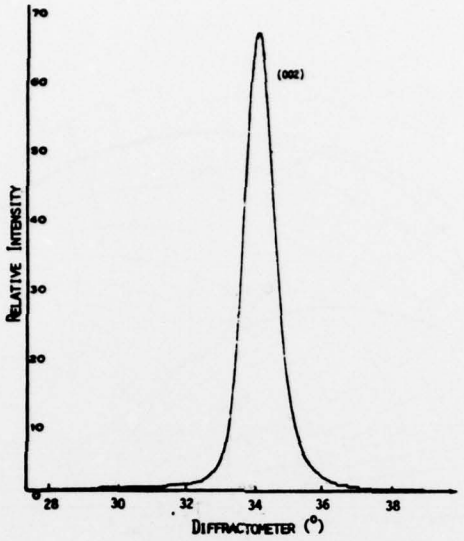

Figure 7. X-Ray Diffractometer Data for a Highly Oriented ZnO Film on Glass Substrate (c-axis normal to surface)

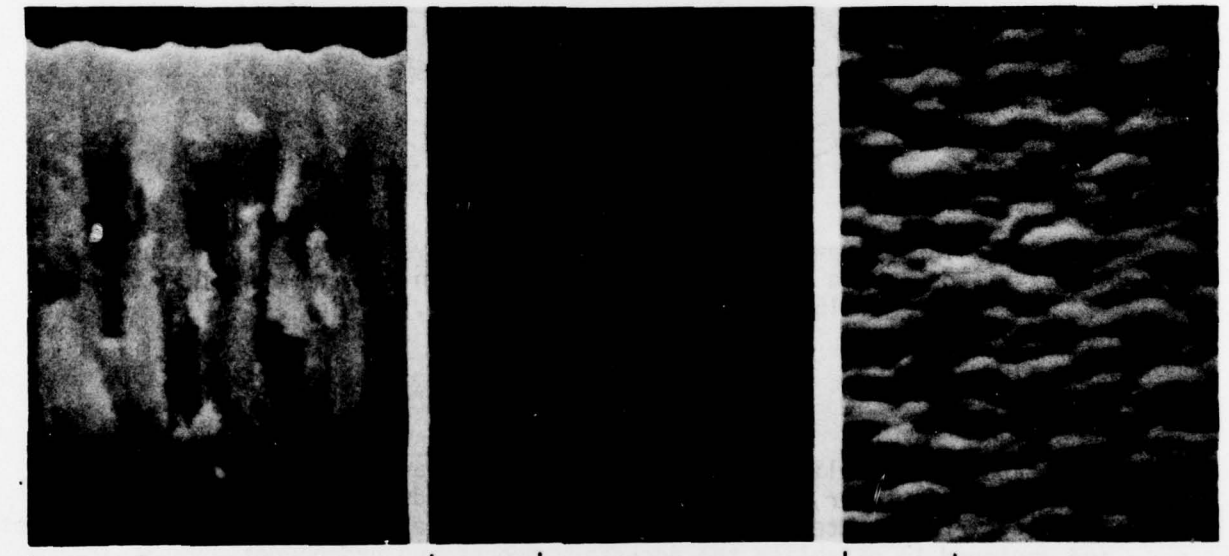

Cleaved Edge

Upper Surface of Sample #106
Grain Size: ≤ 0.5μ; Mean ∿ 0.25μ

Upper Surface of Sample #102
Grain Size: ≤ 1μ; Mean ∿ 0.5μ

Figure 8. Scanning Electron Micrographs RF-Sputtered ZnO on Corning 7440 Glass

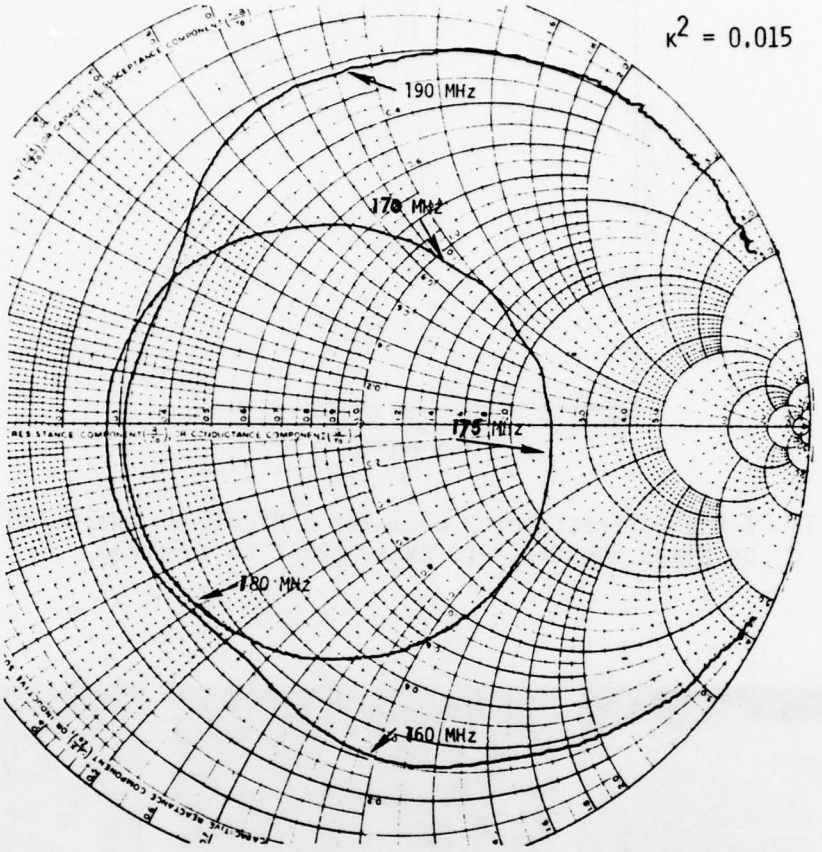

Figure 9. Input Impedance of Surface Elastic Wave Interdigital Transducer on ZnO on a Glass Substrate Showing an Electromechanical Coupling k^2 = 0.015 Where the ZnO Overlay is 6.1μ Thick

RESULTS

Gadolinium gallium garnet fibers without cladding were supplied from another manufacturer via NRL for this effort. Additional fibers with cladding were expected. The initial supply was examined by various techniques and employed to establish the necessary processing procedures.

The fibers were examined for optical clarity. This test was performed by placing an index matching fluid on one end of the as-received fiber and focusing radiation from an He/Ne laser at 6328 Å on the end. The results of this test showed numerous scattering centers along the length of the fiber. The scattering centers indicate either the presence of impurities and/or crystalline discontinuities. Transverse microscopic examination along the fiber length show the presence of fractures which run through all but

approximately 3 centimeters in length. Scanning electron microscopy indicated fracturing which extended beyond the region that could be observed under optical microscopy. Examination of the optical properties under crossed polarization revealed the presence of twinning in the fibers and stress patterns along the entire length. Comparison with bulk G^3 slices sliced and polished to remove damage and displaced from the seed shows no comparable effects.

The crystals exhibited very little compliance. Flexure introduced splitting longitudinally along the fiber. Representative photographs of these results were provided to NRL under separate cover.

To support the results observed optically, X-ray work was performed on the fibers to determine crystalline quality. A representative sample was mounted on a Debye-Scherrer camera. The fibers were drawn in the <100> crystalline direction. One exposure was made while the specimen was stationary. Others were made while it was rotating. The results of these data indicate the fibers are composed of large-grain single crystals (approximately 100 microns), but some crystallites extend to a millimeter. It was concluded from this data that the crystalline quality was marginal for elastic wave devices, that is, the grain boundaries and fractures would act as internal reflectors. The fiber exterior surfaces exhibited growth rings typical of the Czochralski process.

These fibers were polished by modification of standard techniques developed in the Electronics Research Center for polishing of gadolinium garnet substrates for magnetic bubble domain epitaxy. The elastic wavelength defines the requirement for a high degree of parallelism of the ends, planarity of the surfaces, and orthoganality to the fiber axis. The capillary internal diameter was matched to the garnet fiber. The capillary was cut longitudinally in some cases. A soluble epoxy was employed for binding. Problems were encountered during the polishing which are related to the crystalline imperfection. When grain boundaries were encountered, the polishing rate differed from one grain to another. When a fracture was exposed at the end, it allowed the polishing medium to collect in the fracture. It then periodically released and travelled across the surface introducing scratches.

Figure 10 shows two representative examples of the polished end of the support capillary encapsulating epoxy and garnet fiber. The granular finish is representative of the completion of the abrasive lapping process. Normally, a chemo-mechanical process would follow. Note the fragmentation of the garnet fiber cross section. The encapsulating epoxy has been filled with alumina to minimize the differences in hardness to obtain a more uniform surface. As can be seen from the photograph, the garnet fiber apparent hardness is less than that of the fused silica, while the lapped epoxy features remain similar to the fused silica capillary. Ultimately, several polished ends were achieved, and two fibers were returned as representative of the results.

Several of the polished garnet fibers were used to fabricate transducers. An electrode of 50 Å of Ti for adhesion followed by an additional 500 Å of Au was applied by evaporation to the end of the garnet while encapsulated. RF

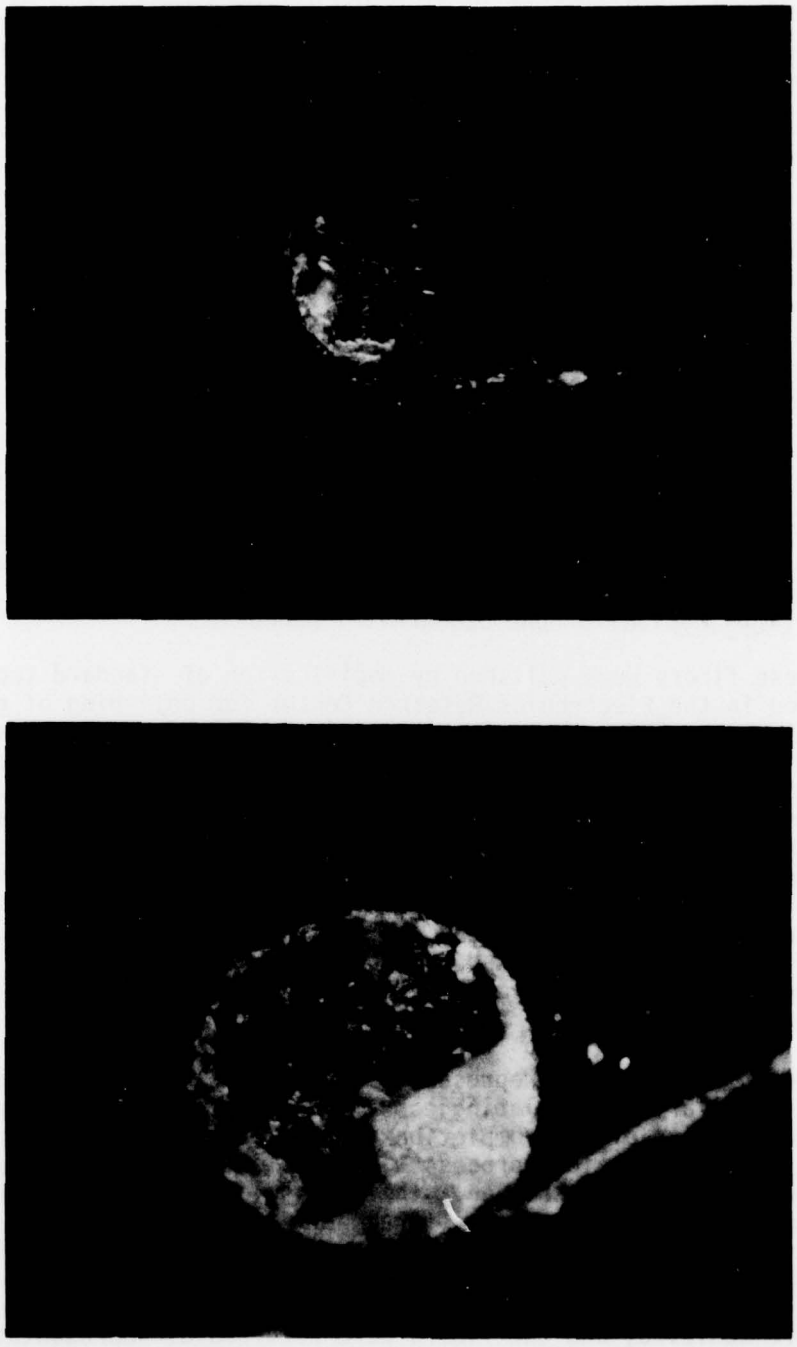

Figure 10. Photographs of Final Lap Surface of Garnet Fiber Encapsulated in Alumina-Loaded Epoxy Contained in Fused Silica Capillary Tube Showing Representative Cross Sections of Garnet Fibers.

sputtered ZnO was applied followed by another electrode which would excite primarily a longitudinal mode. An electromechanical coupling of $k^2 = 1.4 \times 10^{-2}$ was observed. However, no reflected echo was observed, presumably due to the elastic absorption of the bonding of the encapsulated epoxy and because the fibers did not include a cladding for isolation.

These results were reported orally together with photographs of completed polished ends together with polished fibers to the cognizant authority at the Naval Research Laboratory. As a result, further effort was tabled pending receipt of improved garnet fibers.

RECOMMENDATIONS

Based upon this experience and the current availability of large G^2 substrates with magnetic overlay films suggests that an alternate approach could be pursued as delay lines confined to a garnet half surface. The crystallographic quality of this type of structure derived from the liquid epitaxy is known to be nearly entirely defect free as required by bubble domain memory applications.

CONCLUSION

This effort was completed by the preparation of assorted transducer masks prepared and delivered in accordance with NRL drawings 48-2013-60, 48-2014-60 and 48-0009-60.

REFERENCES

1. R. L. Rosenberg, R. V. Schmidt, and L. A. Coldren, "Interior-Surface Acoustic Waveguiding in Capillaries," Appl. Phys. Lett. 25, 324 (1974).

2. G. D. Boyd, L. A. Coldren, and R. N. Thurston, "Acoustic Waveguide with a Cladded Core Geometry," Appl. Phys. Lett. 26, 31 (1975).

3. R. A. Waldron, "Some Problems in the Theory of Guided Microsonic Waves," IEEE Trans. on Microwave Theory and Techniques MTT-17, 893 (1969).

4. B. A. Auld, "Acoustic Fields and Waves in Solids," Vol. I and II, J. Wiley, New York, 1973.

5. T. M. Reeder, D. K. Winslow, "Characteristics of Microwave Acoustic Transducers for Volume Wave Excitation," IEEE Trans. on Microwave Theory and Techniques MTT-17, 927 (1969).

6. D. W. Oliver and G. A. Slack, "Ultrasonic Attenuation in Insulators at Room Temperature," J. Appl. Phys. 37, 1542 (1966).

7. E. G. Spencer, R. T. Denton, T. B. Bateman, W. B. Snow, and L. G. Van Uitert, "Microwave Elastic Properties of Nonmagnetic Garnets," J. Appl. Phys. 34, 3059 (1963).

8. L. J. Graham and R. Chang, "Elastic Moduli of Single-Crystal Gadolinium Gallium Garnet," J. Appl. Phys. 41, 2247 (1970).

9. M. Dutoit and D. W. Bellavance, "Ultrasonic Attenuation Measurements in Gadolinium Gallium Garnet," 1972 Ultrasonics Symposium Proceedings, 136.

10. R. N. Thurston, Torsional Acoustic Modes in a Clad Rod," IEEE Trans. on Sonics and Ultrasonics SU-23, 154 (1976).

11. R. M. Malbon, D. J. Walsh, and D. K. Winslow, "Zinc-Oxide Film Microwave Acoustic Transducers," Appl. Phys. Lett. 10, 9 (1967).

12. N. F. Foster, G. A. Coquin, G. A. Rozgonyi, and F. A. Vannatta,"Cadmium Sulphide and Zinc Oxide Thin-Film Transducers," IEEE Trans. on Sonics and Ultrasonics SU-15, 28 (1968).

13. A. H. Fahmy and E. L. Adler, "Structure and Properties of RF Sputtered ZnO Transducers," IEEE Trans. on Sonics and Ultrasonics SU-19, 346 (1972).

14. F. S. Hickernell, "Zinc-Oxide Thin-Film Surface-Wave Transducers," Proc. IEEE 64, 631 (1976).

15. D. L. Denburg, "Wide-Bandwidth High-Coupling Sputtered ZnO Transducers on Sapphire," IEEE Trans. on Sonics and Ultrasonics SU-18, 31 (1971).

16. N. F. Foster, "Crystallographic Orientation of Zinc Oxide Films Deposited by Triode Sputtering," Vac. Sci. & Tests J. 6, 111 (1969).

17. R. Wagers, G. Kino, P. Galle, and D. Winslow, "ZnO Acoustic Transducers Utilizing Crystalline Gold Substrata," 1972 Ultrasonics Symposium Proc., 194.

18. G. L. Dybwad, "C-Axis Orientation of Sputtered ZnO Films," J. Appl. Phys. 42, 5192 (1971).

19. F. S. Hickernell, "DC Triode Sputtered Zinc Oxide Surface Elastic Wave Transducers," J. Appl. Phys. 44, 1061 (1973).

20. N. F. Foster, "Performance of Shear Mode Zinc Oxide Thin-Film Ultrasonic Transducers," J. Appl. Phys. 40, 4202 (1969).

21. M. Minakata, N. Chubachi, and Y. Kibuchi, "Variation of c-Axis Orientation of ZnO Thin Films Deposited by DC Diode Sputtering," J. Appl. Phys. 12, 474 (1973).

22. J. A. Thornton, "Influence of Apparatus Geometry and Deposition Conditions on the Structure and Topography of Thick Sputtered Coatings," J. Vac, Sci. Technol. 11, 666 (1974).

23. D. L. Denburg and G. L. Dybwad, "Diagnostic Rate Monitoring of Sputtered ZnO Films, J. Appl. Phys. 44, 2724 (1973).